Evaluating Degree of Freedom Selection Methods for MIMO Vibration Modeling

Moheimin Khan[1], Tyler Schoenherr[1]

[1]Sandia National Laboratories, P.O. Box 5800 – MS0346, Albuquerque, NM, 87185

ABSTRACT
Multiple-input multiple-output (MIMO) vibration testing techniques offer the ability to closely replicate field environments during ground testing in a cost-effective manner, often with significant time savings compared to single-axis methods. MIMO techniques have been successfully applied to vibration testing for aerospace applications, yet they are also useful for providing inputs for the model validation process. However, choosing appropriate sensor locations and degrees of freedom (DOF) is an important but challenging aspect of the MIMO approach. This work highlights the application of MIMO techniques to perform model validation for an example aerospace system using synthetic test data. An inverse approach is utilized to perform input estimation, with frequency response functions and simulated acceleration response data from a finite element model. To assess the quality of the input estimation, several selection techniques for MIMO are evaluated, including those based on effective independence, optimal experimental design, modal projection error, and an iterative approach based on mean-squared error. This work demonstrates the development of a workflow for model validation of an aerospace system using the application of MIMO techniques, emphasizing the importance of control DOF selection and showcasing advantages over single-axis methods.
Keywords: MIMO, vibration, sensor, model validation, environments

INTRODUCTION

Multiple-input multiple-output (MIMO) techniques have increased in popularity over the last decade, especially in the area of experimental structural dynamics. In aerospace applications, MIMO can be used during vibration ground testing to recreate the response of a system to its operating or field environment. Multi-axis techniques offer the ability to replicate field response at multiple locations of interest, often with lower forces compared to single-axis testing. Multiple electrodynamics shakers have been used in various configurations, starting with the 6 degree-of-freedom (DOF) shaker system, which demonstrated an improved method for base excitation [1]. Another development in MIMO applications was impedance-matched multi-axis testing (IMMAT) [2], in which individual shakers are arranged to recreate field response by closely simulating the dynamic impedance of the next-level assembly. Other techniques focus on providing input forces directly at the system boundary or intrinsic connection points [3]. Regardless of the technique, MIMO has several advantages over traditional single-input single-output (SISO) testing. Most notably, exciting the test article in a more representative field environment improves the ability of ground testing to predict in-service structural performance.

The same techniques that are used to closely simulate response to field environments in the laboratory can also be directly utilized in the model validation process. For example, responses from a finite element (FE) model can be directly compared to test data measured in the lab. By applying MIMO principles to analytical models, current approaches to model validation can be improved. Instead of relying on the response of a single control degree of freedom or using the test input specification and propagating model form error, MIMO techniques can be used to improve inputs to the FE model that better match the test conditions. In the same way that MIMO tests aim to recreate the field response, MIMO modeling can better recreate testing conditions and also help with test planning.

MIMO modeling can be used to evaluate the accuracy of FE models, compare system dynamics between model and test, assess

model boundary conditions, and evaluate responses at unmeasured locations. This work uses synthetic test data to demonstrate the application of MIMO approaches to model validation, utilizing the FE model in combination with the synthetic test data. Specifically, the model modes are used to calculate frequency response functions and input estimation is performed to compute the forces required to best match synthetic test data. A commonly used tool to calculate the input force is the pseudo-inverse, which minimizes the least-squares error to the test response.

The MIMO estimation process starts with the simple input-output relationship for a linear time-invariant dynamic system. In the frequency domain, this can be expressed as

$$Y(\omega) = H_{yx}(\omega)X(\omega) \tag{1}$$

Here, the linear response spectrum $Y(\omega)$ is computed using the system frequency response function (FRF) $H_{yx}(\omega)$ and the input spectrum $X(\omega)$. For random vibration problems, it is advantageous to use the power space representation to obtain the following relationship:

$$S_{yy}(\omega) = H_{yx}(\omega)S_{xx}(\omega)H_{yx}(\omega)^{\mathrm{H}} \tag{2}$$

Here, the output cross-power spectral density (CPSD), $S_{yy}(\omega)$, is equal to the input CPSD, $S_{xx}(\omega)$, pre-multiplied by the system FRF and post-multiplied by its complex conjugate transpose or Hermitian, designated by $(.)^{\mathrm{H}}$.

The objective of the MIMO input estimation is to determine the input model loads $S_{xx2}(\omega)$, which make the system $H_{yx2}(\omega)$ respond as $S_{yy2}(\omega)$, to best match the lab response, $S_{yy1}(\omega)$. The process can be outlined as follows:

1. Obtain test data at locations of interest, $S_{yy1}(\omega)$
2. Use model FRF, $H_{yx2}(\omega)$, and compute pseudo-inverse (shown as $(.)^{+}$) to determine input load that best fits test response

$$S_{xx2}(\omega) = H_{yx2}(\omega)^{+}S_{yy1}(\omega)H_{yx2}(\omega)^{+\mathrm{H}} \tag{3}$$

3. Solve the forward problem by calculating the updated model response, $S_{yy2(\omega)}$

$$S_{yy2}(\omega) = H_{yx2}(\omega)S_{xx2}(\omega)H_{yx2}(\omega)^{\mathrm{H}} \tag{4}$$

Ideally, the model response would be approximately equal to the test response at all locations of interest: $S_{yy2}(\omega) \approx S_{yy1}(\omega)$. However, the pseudo-inverse computation in Equation 3 provides a least-squares solution to the entire CPSD, which can result in poor matches for some individual DOF and is sensitive to the relative number of inputs and outputs. Thus, it is imperative to select appropriate input and output DOF to obtain the desired accuracy in matching responses, while also representing global dynamic response. Considering DOF not part of the input or control, known as a validation set, is one way to evaluate the quality of the MIMO solution.

In the case of the 6DOF shaker table, the input DOF are known so the challenge remains in selecting the resulting control locations for MIMO vibration. Many methods exist to aid with DOF selection and a variety of objectives can be considered. This work investigates DOF selection through effective independence [4], an iterative approach based on mean squared error [5], optimal experimental design [6] [7], and modal projection error [8]. The application of these techniques to MIMO vibration of an aerospace structure is demonstrated in this work. Synthetic data is generated using a finite element model and comparative results are presented, including quantitative metrics used to evaluate the quality of the resulting control set.

MODELING

The aerospace system of interest studied in this work is the Wedding Cake and Removable Component Assembly (WRCA) [9], shown in Fig. 1. The structure is an assemblage of research articles and contains adequate dynamic complexity, making it an interesting exemplar for studying MIMO modeling techniques. An FE model of the WRCA was created using computational tools developed at Sandia National Laboratories, including CUBIT [10] and Sierra/SD [11]. Details are provided in [9].

Due to the unavailability of test data to demonstrate the MIMO process outlined previously, synthetic data was generated for the WRCA. This synthetic test data was created by modifying the baseline FE model with adjusted material properties and also removing a selection of the ”test” modes. By doing so, the dynamics of the WRCA test and model configurations are sufficiently different, simulating typical modeling error when comparing to test data. The modal assurance criterion (MAC) was used to quantify the dynamic differences between the model and synthetic test assembly. For this study, 50 model modes (around 1800 Hz) were used and 5 modes under 1000 Hz were removed from the test configuration. The MAC plot in Fig. 2 illustrates these dynamic differences in the 1 kHz bandwidth of interest.

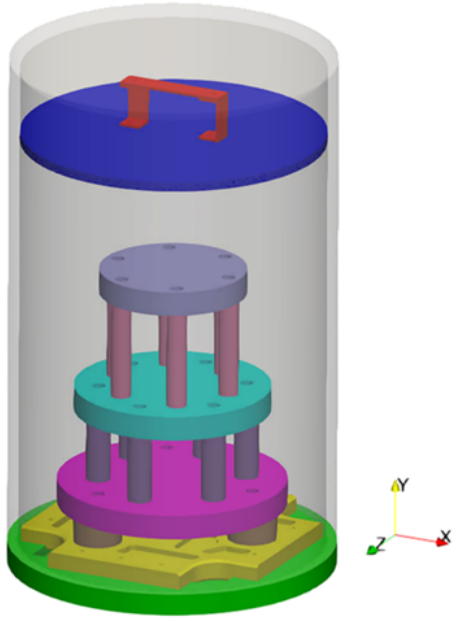

Fig. 1 WRCA model [9]

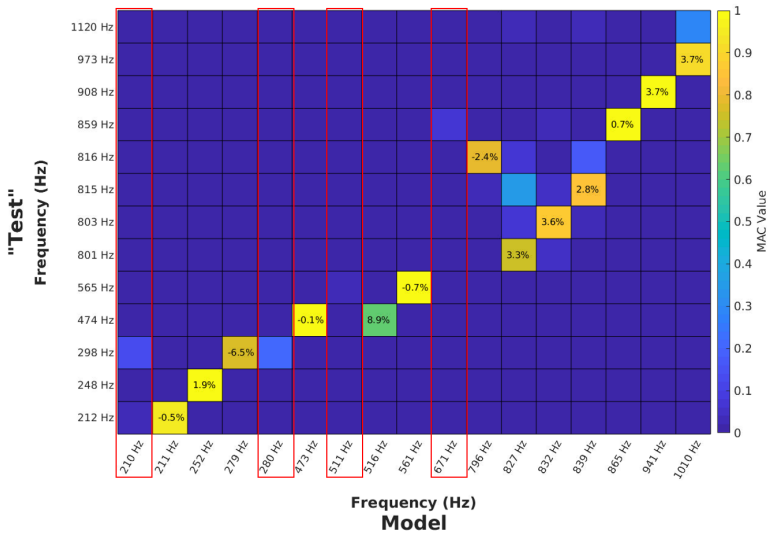

Fig. 2 MAC between synthetic test and model configurations, highlighting removed modes

The MIMO modeling approach used in this work uses a least-squares, pseudo-inverse calculation as its foundation. A workflow was developed in MATLAB to utilize the model mode shapes at the locations of interest, compute frequency response functions (FRFs), and perform the MIMO input estimation using target synthetic test data. A synthetic test environment for the WRCA was generated by applying a single-axis base input in the transverse +Z direction.

For a given set of test and model data, the most important parameters used in the MIMO workflow are the input and output (control) DOF. For the WRCA, a set of 48 points (144 DOF) were used as candidate locations for the down-selection process. Additionally, 12 validation DOF were used to check the response at important locations outside the input and control set, and to assess the quality of the MIMO solution. Figure 3 shows the initial candidate and validation point locations.

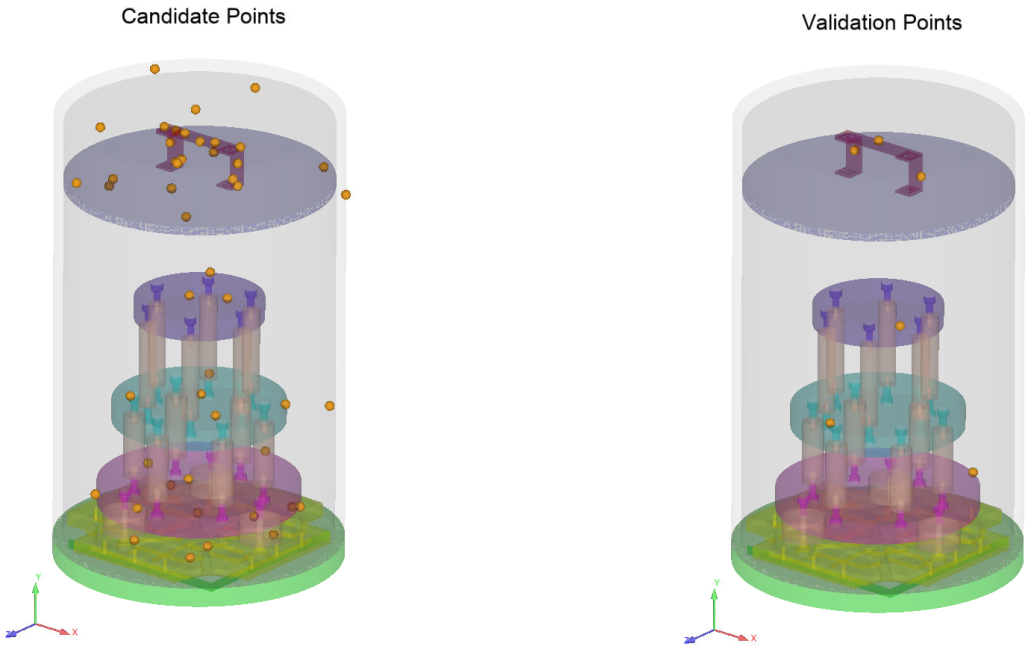

(a) **(b)**

Fig. 3 Candidate (a) and validation (b) locations

Case studies were performed using a variety of DOF selection approaches covered in the literature. Simulations were completed using both single and multi-axis input and control techniques. The input estimation was performed using the generated synthetic test data and a total of 5 separate modeling approaches:

1. Traditional single-input single-output (SISO) loading, using base input and single control DOF on the RC
2. 6DOF base input with effective independence (EI) [4] to down-select the number of control DOF
3. 6DOF base input using an iterative mean-squared error (MSE) approach [5] to down-select the number of control DOF
4. 6DOF base input using an optimal experimental design (OED) greedy algorithm (D-optimality) [5], [7] to down-select the number control DOF
5. 6DOF base input using modal projection error (MPE) [8] to down-select the number of control DOF

For each of the MIMO DOF selection methods, two separate cases were considered to assess the influence of control DOF size: (1) a subset of 12 DOF and (2) a subset of 50 DOF from the original 48-point, 144 DOF candidate set shown in Fig. 3a. For each case, the results were compared by computing a summation of the auto-power spectral density (APSD) acceleration response for the validation points shown in Fig. 3b. Quantitative metrics including maximum dB error, average dB error, and computational time were also considered. Results are detailed in the following section.

RESULTS

Figure 4 illustrates the down-selected locations and orientations for each MIMO method for the 12 DOF case. Fig. 7 in the Appendix shows the 50 DOF case for reference. As outlined previously, 6DOF base inputs were computed for each method using the down-selected DOF for each case, and the sum APSD response of the validation points was computed to assess the match to the synthetic test data. Fig. 5 shows the plotted APSD sum for the validation points for the 12 and 50 DOF cases.

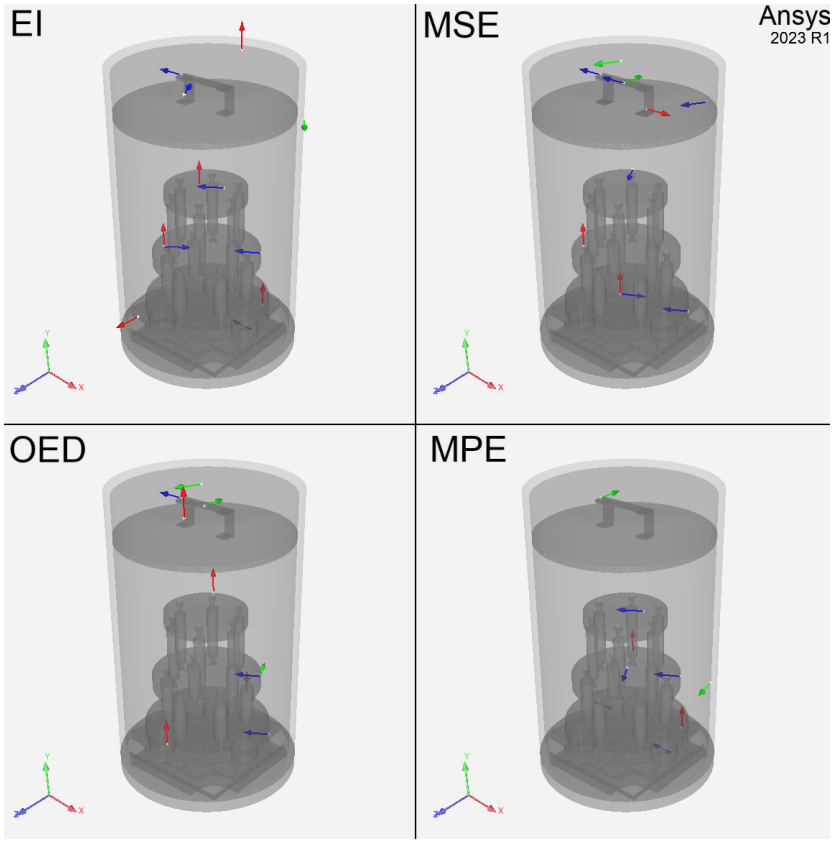

Fig. 4 Comparison of down-selected control DOF for each method (12 DOF)

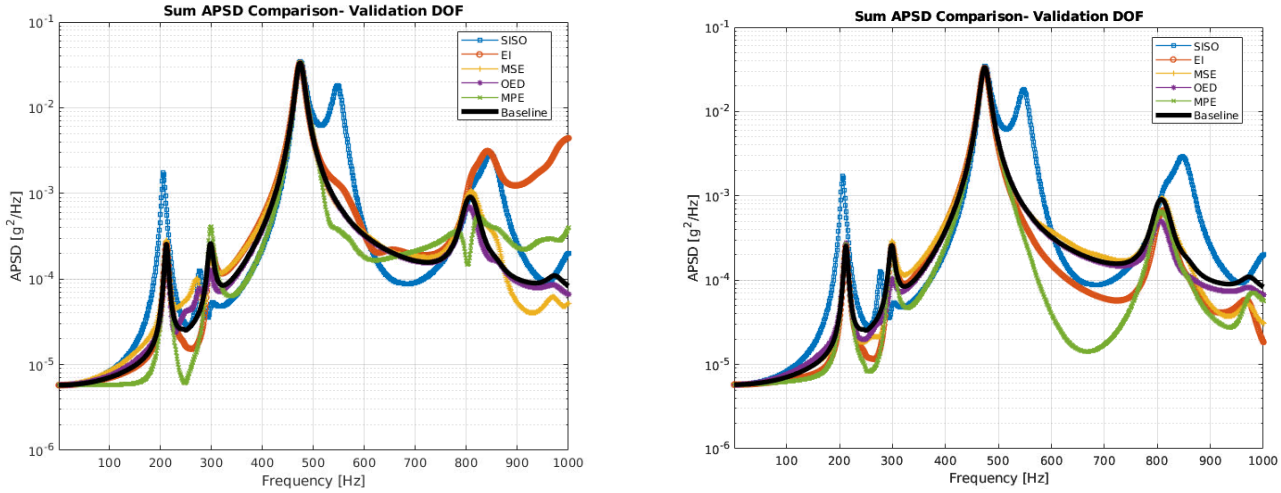

(a) **(b)**

Fig. 5 ASD comparison for 12 (a) and 50 (b) control DOF cases

Additionally, Fig. 6 displays the maximum and root-mean-square (RMS) dB error for each result plotted in Fig. 5. A summary of the computational time for each case is also provided in Table 1.

Starting with the 12 DOF case in Fig. 5a, it is apparent that the SISO method has the largest deviation from the test response, especially at the peaks. Since the method is limited to a single input and control, there is no compensation in the input for the dynamic differences between the model and test cases, which leads to the overshoot at the peaks near 200, 550, and 850 Hz. The rest of the methods match the validation DOF response well, except at higher frequencies, where EI and MPE deviate due to the restriction of modal truncation. Both EI and MPE require the number of DOF to be greater than or equal to the number of modes used in the selection process. Looking at the increased number of control DOF in Fig. 5b, the two mode shape-based methods match better at the peak response and at higher frequencies due to the inclusion of additional modes. However, both perform worse at the anti-resonances, especially MPE between 550 and 750 Hz. On the other hand, MSE and OED maintain an excellent match for this case and appear to have the best overall fit for the validation DOF.

Figure 6 further illustrates the relative performance of each method. In general, SISO has the highest maximum and RMS error, except for the EI 12 DOF and MPE 50 DOF case. MSE and OED have both have the lowest overall error, performing similarly for maximum dB error, and OED having the lowest RMS dB error. To further distinguish each method, it is also interesting to study the computational cost (normalized to the SISO case), summarized in Table 1. Though MSE and OED both perform well, the iterative and computationally intensive nature of MSE causes it to be anywhere from 1 to 2 orders of magnitude slower than the other methods. The rest of the techniques require approximately the same amount of time, although MPE also increases in computational cost as the number of modes increases.

Overall, OED appears to be the best DOF selection method for the cases studied. MSE also provides good results, although the high computational cost may make it difficult to use depending on the size of the problem. EI and MPE also do well compared to the SISO case, but results are dependent on the number of modes in the model relative to control DOF size. The required model inputs used for each method varies as well, with EI and MPE using only the mode shapes, OED requiring the FRF, and MSE needing the full APSD for each DOF. These results are also problem-dependent, but give an idea of the available methods, showcasing the advantages and disadvantages and highlighting the benefit of MIMO modeling approaches in better replicating the overall test response.

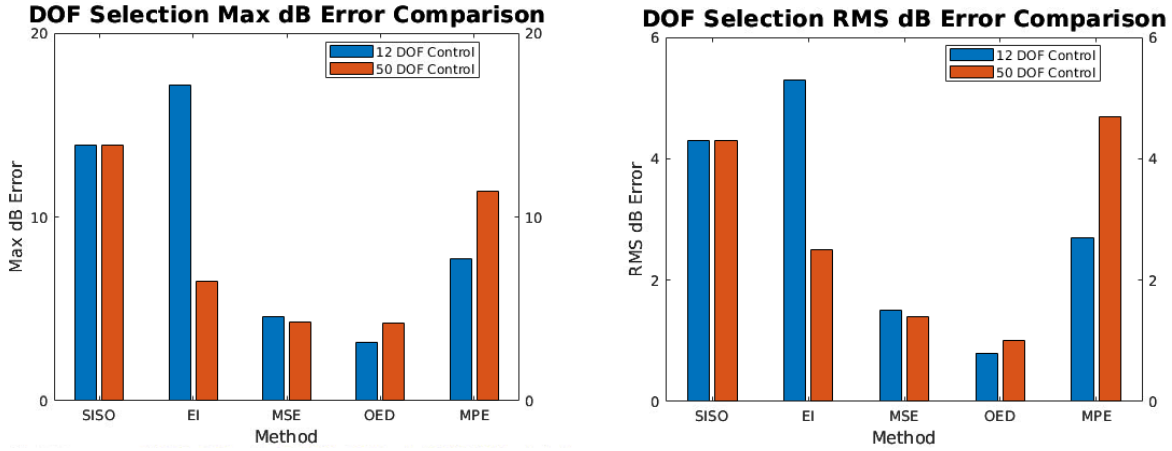

(a) **(b)**

Fig. 6 Maximum (a) and RMS (b) dB error for each method

Table 1: Summary of method performance

Method	Normalized computational cost, 12 DOF	Normalized computational cost, 50 DOF
SISO	1.0	1.0
EI	1.2	1.6
MSE	111.5	95.1
OED	1.3	1.9
MPE	1.5	9.6

CONCLUSIONS

This work highlighted the use of MIMO techniques for model validation of an aerospace system using synthetic test data. Input estimation was performed using simulated acceleration response data from a finite element model. Several DOF selection techniques for MIMO were evaluated, with objectives based on effective independence, mean-squared error, optimal experimental design, and modal projection error. Results showed a good match to synthetic test data using MIMO methods and a demonstrable improvement over typical SISO methodology. Mean-squared error (MSE) and optimal experimental design (OED) methods gave the best matches overall, although MSE may be limited by its high computational cost. The work demonstrates the development of a workflow for model validation of an aerospace system using the application of MIMO techniques, emphasizing the importance of control DOF selection and showcasing advantages over single-axis methods. Future work will investigate additional selection methods, including the effect of input DOF. In addition, further studies will be performed using experimental test data and incorporating calibrated models in the MIMO input estimation process.

ACKNOWLEDGMENTS

I would like to acknowledge and thank everyone who helped me along the way. B. Zwink for the discussions on MIMO and sharing similar work on the topic. And those who guided me as I learned about MIMO and sensor selection techniques, including R. Schultz, C. Beale, D. Rohe, J. Wilbanks, and C. Smith.

Sandia National Laboratories is a multi-mission laboratory managed and operated by National Technology & Engineering Solutions of Sandia, LLC (NTESS), a wholly owned subsidiary of Honeywell International Inc., for the U.S. Department of Energy's National Nuclear Security Administration (DOE/NNSA) under contract DE-NA0003525. This written work is authored by an employee of NTESS. The employee, not NTESS, owns the right, title and interest in and to the written work and is responsible for its contents. Any subjective views or opinions that might be expressed in the written work do not necessarily represent the views of the U.S. Government. The publisher acknowledges that the U.S. Government retains a non-exclusive, paid-up, irrevocable, world-wide license to publish or reproduce the published form of this written work or allow others to do so, for U.S. Government purposes. The DOE will provide public access to results of federally sponsored research in accordance with the DOE Public Access Plan. `https://www.energy.gov/downloads/doe-public-access-plan`

REFERENCES

[1] D. O. Smallwood and D. L. Gregory, "Evaluation of a six-dof electrodynamic shaker system," in *Proc. 79th Shock and Vibration Symp.*, Orlando, FL, 2008.

[2] P. Daborn, P. Ind, and D. Ewins, "Enhanced ground-based vibration testing for aerodynamic environments," *Mechanical Systems and Signal Processing*, vol. 49, no. 1, pp. 165–180, 2014, ISSN: 0888-3270. DOI: https://doi.org/10.1016/j.ymssp.2014.04.010. [Online]. Available: https://www.sciencedirect.com/science/article/pii/S0888327014001162.

[3] B. Zwink, K. Cross, and D. Fowler, "Mimo vibration test design for barc challenge problem," in *Proc. International Modal Analysis Conference (IMAC 41)*, Austin, TX, 2023.

[4] D. C. Kammer, "Sensor placement for on-orbit modal identification and correlation of large space structures," *Journal of Guidance, Control, and Dynamics*, vol. 14, no. 2, pp. 251–259, 1991. DOI: 10.2514/3.20635. eprint: https://doi.org/10.2514/3.20635. [Online]. Available: https://doi.org/10.2514/3.20635.

[5] C. Beale, R. Schultz, C. Smith, and T. Walsh, "Degree of freedom selection approaches for mimo vibration test design," All Open Access, Green Open Access, 2023, pp. 81–90. DOI: 10.1007/978-3-031-05405-1_10. [Online]. Available: https://www.scopus.com/record/display.uri?eid=2-s2.0-85135793056&origin=inward&txGid=2dbe3bb5f50f34411878009e6457f84e.

[6] D. Ridzal, D. P. Kouri, and G. J. von Winckel, "Rapid optimization library.," Nov. 2017. [Online]. Available: https://www.osti.gov/biblio/1481491.

[7] V. Akcelik, W. Aquino, A. Kurzawski, *et al.*, "Inverse methods - users manual 5.8," Jun. 2022. DOI: 10.2172/1874427. [Online]. Available: https://www.osti.gov/biblio/1874427.

[8] T. F. Schoenherr and J. W. Rouse, "Characterizing dynamic test fixtures through the modal projection error," *Mechanical Systems and Signal Processing*, vol. 204, p. 110 746, 2023, ISSN: 0888-3270. DOI: https://doi.org/10.1016/j.ymssp.2023.110746. [Online]. Available: https://www.sciencedirect.com/science/article/pii/S0888327023006544.

[9] M. Khan, J. Wilbanks, C. Smith, T. Walsh, and B. Owens, "Comparing Instrumentation Selection Techniques for Vibration Testing," *ASME Letters in Dynamic Systems and Control*, vol. 2, no. 4, p. 040 901, Oct. 2022, ISSN: 2689-6117. DOI: 10.1115/1.4055765. eprint: https://asmedigitalcollection.asme.org/lettersdynsys/article-pdf/2/4/040901/6931980/aldsc_2_4_040901.pdf. [Online]. Available: https://doi.org/10.1115/1.4055765.

[10] C. Stimpson, G. Sjaardema, C. Dudley, *et al.*, *Cubit v.16.x*, [Computer Software], Aug. 2022. DOI: 10.11578/dc.20221017.1. [Online]. Available: https://doi.org/10.11578/dc.20221017.1.

[11] D. Beale, G. Bunting, M. Chen, *et al.*, "Sierra/sd - user's manual - 5.6," Sandia National Laboratories, Report SAND2022-3498, Mar. 2022. [Online]. Available: https://www.osti.gov/biblio/1856667-sierra-sd-user-manual.

APPENDIX

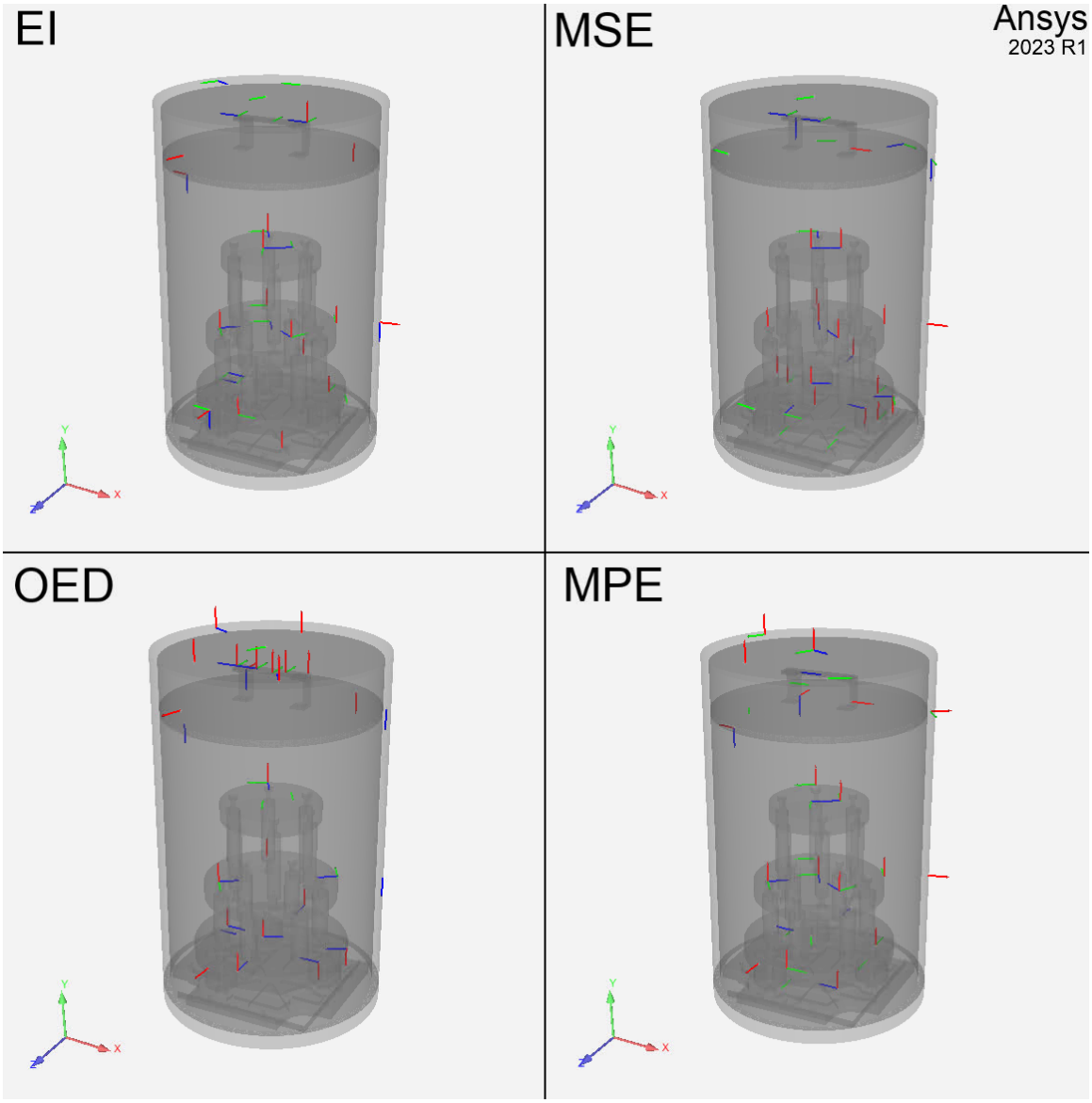

Fig. 7 Comparison Down-Selected Control DOF for Each Method (50 DOF)